UC Irvine

UC Irvine Previously Published Works

Title

A multi-epitope/CXCL11 prime/pull coronavirus mucosal vaccine boosts the frequency and the function of lung-resident memory CD4+ and CD8+ T cells and enhanced protection against COVID-19-like symptoms and death caused by SARS-CoV-2 infection.

Permalink

https://escholarship.org/uc/item/7t85z39k

Journal

Journal of Virology, 97(12)

Authors

Zayou, Latifa
Prakash, Swayam
Dhanushkodi, Nisha
et al.

Publication Date

2023-12-21

DOI

10.1128/jvi.01096-23

Peer reviewed

eScholarship.org Powered by the California Digital Library
University of California

Journal of Virology

Vaccines | Full-Length Text

A multi-epitope/CXCL11 prime/pull coronavirus mucosal vaccine boosts the frequency and the function of lung-resident memory CD4$^+$ and CD8$^+$ T cells and enhanced protection against COVID-19-like symptoms and death caused by SARS-CoV-2 infection

Latifa Zayou,[1,2] Swayam Prakash,[1] Nisha Rajeswari Dhanushkodi,[1] Afshana Quadiri,[1] Izabela Coimbra Ibraim,[3] Mahmoud Singer,[1] Amirah Salem,[1] Amin Mohammed Shaik,[1] Berfin Suzer,[1] Amruth Chilukuri,[1] Jennifer Tran,[1] Pauline Chau Nguyen,[1] Miyo Sun,[1] Kathy K. Hormi-Carver,[1] Ahmed Belmouden,[2] Hawa Vahed,[4] Daniel Gil,[4] Jeffrey B. Ulmer,[4] Lbachir BenMohamed[1,4,5,6]

AUTHOR AFFILIATIONS See affiliation list on p. 15.

ABSTRACT The pandemic of the coronavirus disease 2019 (COVID-19) has created the largest global health crisis in almost a century. Low frequencies of functional SARS-CoV-2-specific CD4$^+$ and CD8$^+$ T cells in the lungs of COVID-19 patients have been associated with severe cases of COVID-19. Low levels of T cell-attracting CXCL9, CXCL10, and CXCL11 chemokines in infected lungs may not be sufficient for the migration of CD4$^+$ and CD8$^+$ T cells from circulation into infected lungs. We hypothesize that a coronavirus vaccine strategy that boosts the frequencies of functional SARS-CoV-2-specific CD4$^+$ and CD8$^+$ T cells in the lungs would lead to better protection from COVID-19-like symptoms. In the present study, we designed and pre-clinically tested the safety, immunogenicity, and protective efficacy of a novel multi-epitope/CXCL11 prime/pull mucosal coronavirus vaccine. This prime/pull vaccine strategy consists of intranasal delivery of a lung-tropic adeno-associated virus type 9 vector that incorporates highly conserved human CD4$^+$ and CD8$^+$ cell epitopes of SARS-CoV-2 (*prime*) followed by recruitment of the primed T cells into the lungs using the T cell-attracting chemokine, CXCL-11 (*pull*). We demonstrated that the immunization of HLA-DR*0101/HLA-A*0201/hACE2 triple transgenic mice with this multi-epitope/CXCL11 prime/pull coronavirus mucosal vaccine: (i) increased the frequencies of functional CD4$^+$ and CD8$^+$ T_{EM}, T_{CM}, and T_{RM} cells in the lungs and (ii) reduced COVID-19-like symptoms, lowered virus replication, and prevented deaths following challenge with SARS-CoV-2. These findings demonstrate that bolstering the number of functional lung-resident memory CD4$^+$ and CD8$^+$ T cells improved protection against SARS-CoV-2 infection, COVID-19-like symptoms, and death.

IMPORTANCE Although the current rate of SARS-CoV-2 infections has decreased significantly, COVID-19 still ranks very high as a cause of death worldwide. As of October 2023, the weekly mortality rate is still at 600 deaths in the United States alone, which surpasses even the worst mortality rates recorded for influenza. Thus, the long-term outlook of COVID-19 is still a serious concern outlining the need for the next-generation vaccine. This study found that a prime/pull coronavirus vaccine strategy increased the frequency of functional SARS-CoV-2-specific CD4$^+$ and CD8$^+$ memory T cells in the lungs of SARS-CoV-2-infected triple transgenic HLA-DR*0101/HLA-A*0201/hACE2 mouse model, thereby resulting in low viral titer and reduced COVID-19-like symptoms.

KEYWORDS SARS-CoV-2, COVID-19, memory CD4$^+$, CD8$^+$ T cells, CXCL-11, lungs

Editor Paul G. Thomas, St. Jude Children's Research Hospital, Memphis, Tennessee, USA

Address correspondence to Lbachir BenMohamed, Lbenmoha@uci.edu.

L.B.M. has an equity interest in TechImmune, LLC, a company that may potentially benefit from the research results and serves on the company's Scientific Advisory Board. L.B.M.'s relationship with TechImmune, LLC has been reviewed and approved by the University of California, Irvine, in accordance with its conflict-of-interest policies.

See the funding table on p. 15.

Received 20 July 2023
Accepted 12 November 2023
Published 1 December 2023

Copyright © 2023 American Society for Microbiology. All Rights Reserved.

Severe acute respiratory syndrome coronavirus 2 (SARS-CoV-2), a novel coronavirus identified at the end of 2019, has led to an ongoing global pandemic (1). The SARS-CoV-2 virus belongs to the subgenus sarbecovirus of the genus betacoronavirus, the genus from which two SARS-CoV-2 closely related viruses (SARS-CoV-1 and MERS-CoV) has crossed the species barrier to humans over the past two decades (2, 3). SARS-CoV-2 uses angiotensin-converting enzyme 2 (ACE2) receptors to enter and infect pulmonary alveolar cells (4). This causes the SARS-CoV-2 virus particles to replicate in the lungs, inducing a phenomenon known as "cytokine storm" and potentially causing life-threatening inflammatory lung disease (5).

SARS-CoV-specific $CD4^+$ and $CD8^+$ T cells in the lungs play a critical role in aborting virus replication. However, low frequencies of functional SARS-CoV-2-specific $CD4^+$ and $CD8^+$ T cells in the lungs of COVID-19 patients have been associated with severe COVID-19 cases (6). Three major SARS-CoV-2-specific memory $CD4^+$ and $CD8^+$ T cell subsets [i.e., effector memory (T_{EM}), resident memory (T_{RM}), and central memory (T_{CM})] develop, infiltrate, and sequester in the infected lungs in response to three key T cell-attracting chemokines: CXCL9, CXCL10, and CXCL11 among others and enable primed T cells to relocate to specific sites of infection, such as the lungs (7). In addition, CXCR3, a common chemokine receptor of CXCL-9, CXCL-10, and CXCL-11, is expressed on effector and memory T cells and is responsible for the chemotaxis of T cells within this axis (8, 9). However, the low levels of T cell-attracting chemokines CXCL9, CXCL10, and CXCL11 in the infected lungs of severely ill COVID-19 patients may not be sufficient to ensure the sequestration of $CD4^+$ and $CD8^+$ T_{RM} cells or to guide homing $CD4^+$ and $CD8^+$ T_{EM} and T_{CM} cells from circulation into infected lungs (10).

Parenteral vaccines, administrated intramuscularly or subcutaneously, are often less effective in boosting the frequencies of functional $CD4^+$ and $CD8^+$ T cells in mucosal tissues, including the pulmonary mucosal site of SARS-CoV-2 replication (11, 12). In contrast, mucosal vaccines have the potential to produce both mucosal and systemic T cell immunity (13). In the present study, we hypothesize that a prime/pull vaccine strategy that consists of (i), first, priming SARS-CoV-2-specific B cells, $CD4^+$ T cells, and $CD8^+$ T cells using the engineered lung-tropic adeno-associated virus type 9 (AAV9) vector co-expressing the recently identified immunodominant human $CD4^+$ and $CD8^+$ T cell epitopes (14) (designated in this report as CoV-Vaccine) and delivered intranasally followed by (ii) pulling the "primed" $CD4^+$ T cells and $CD8^+$ T cells into the lungs using CXCL-9, CXCL-10, or CXCL-11 T cell-attracting chemokines delivered intranasally (nose drops), will boost the frequency of functional $CD4^+$ and $CD8^+$ T cells and lead to strong local protective T cell immunity in the lungs against SARS-CoV-2 infection, COVID-19-like symptoms, and death.

Using a rational reverse vaccine engineering approach, we designed and pre-clinically tested the safety, immunogenicity, and protective efficacy of three multi-epitope prime/pull coronavirus mucosal vaccine candidates. These coronavirus mucosal vaccines consist of intranasal delivery of a lung-tropic adeno-associated virus type 9 vector that incorporates highly conserved human B, $CD4^+$ T, and $CD8^+$ T cell epitopes of SARS-CoV-2 (14, 15) that are selectively recognized by the B and T cells from naturally protected asymptomatic (ASYMP) COVID patients (*prime*) and pulling the primed T cells into the mucosal sites of the lungs using the T cell-attracting chemokines CXCL-9, CXCL-10, or CXCL-11 (*pull*) (16). Furthermore, we demonstrated that immunization of a novel HLA-DR*0101/HLA-A*0201/hACE2 triple transgenic mouse model with a multi-epitope/CXCL11 prime/pull coronavirus mucosal vaccine boosted high frequencies of functional lung-resident $CD4^+$ and $CD8^+$ memory T cells associated with strong protection against SARS-CoV-2 infection, COVID-19-like symptoms, and death.

MATERIALS AND METHODS

Mice

Female K18-hACE2 transgenic mice (8–9 weeks old) were purchased from the Jackson Laboratory (Bar Harbor, ME). K18-hACE2 mice breeding was conducted in the UCI animal facility, where female mice were used at 8–9 weeks. In addition, female HLA-DR*0101/HLA-A*0201/hACE2 triple transgenic mice (8–9 weeks old) were used. The HLA-DR*0101/HLA-A*0201/hACE2 triple transgenic mouse colony was established here at the UCI by cross-breeding K18-hACE2 mice (17) with double transgenic HLA-DR*0101/HLA-A*0201 mice (14). The animal studies were performed at the University of California Irvine and adhered to the Guide for the Care and Use of Laboratory Animals published by the US National Institute of Health. All animal experiments were performed under the approved IACUC protocol # AUP-22-086.

Immunization and CXC chemokine treatment

Groups of female HLA-DR*0101/HLA-A*0201/hACE2 triple transgenic mice (8–9 weeks old) were immunized intranasally on day 0 with the multi-epitope coronavirus vaccine (CoV-Vacc at 2×10^{10} viral particles [VP] per mouse, $n = 35$). The vaccine incorporated highly conserved and immunogenic 16 $CD8^+$ T cell epitopes, 6 $CD4^+$ T cell epitopes, and 9 B cell epitopes. The recombinant murine MIG (CXCL-9), IP-10 (CXCL-10), and I-TAC (CXCL-11) were obtained from PeproTech, USA. The 35 vaccinated mice were divided into 4 groups of 7 mice each. Three groups of immunized mice were treated intranasally with 3 µg of CXCL-9 ($n = 7$), CXCL-10 ($n = 7$), and CXCL-11 ($n = 7$) (3 µg in 20 µL of sterile PBS/mouse) on days 10, 12, 14, 22, 24, and 26 post-immunizations. The remaining fourth group of CoV-Vacc-immunized mice were left untreated ($n = 7$). As a negative control, a fifth group of seven mice received sterile PBS (mock vaccinated and mock treated).

SARS-CoV-2 infection

K18-hACE2 mice were infected intranasally with 1×10^4 pfu of the SARS-CoV-2-USA-WA1/2020 variant delivered in 20 µL sterile PBS (Fig. 1A). Whereas the HLA-DR*0101/HLA-A*0201/hACE2 triple transgenic mice were intranasally infected with 1×10^4 pfu of SARS-CoV-2 (USA-WA1/2020) delivered in 20 µL sterile PBS on day 28 following immunization (Fig. 2B). Mice were monitored daily for death and weight loss till day 14 post-infection (p.i.) on which they were euthanized for virological and immunological studies in the lungs.

Following intranasal infection with SARS-CoV-2 (USA-WA1/2020), HLA-DR*0101/HLA-A*0201/hACE2 triple transgenic mice were monitored daily for disease progression. Subsequently, three mice groups were treated intranasally with 3 µg of the CXCL-9 ($n = 5$), CXCL-10 ($n = 5$), and CXCL-11 ($n = 5$) diluted in sterile PBS. The mock ($n = 5$) group was treated with sterile PBS. The CXCL chemokine treatment was given on days 3, 5, 7, and 9 (p.i.). On days 4 and 8, oropharyngeal swabs were collected for virus RNA copy number measurement. The SARS-CoV-2-infected mice were monitored up to day 14 p.i. for disease, weight loss, and survival. On day 14 p.i., mice were euthanized. All the experiments were repeated twice for validation.

SARS-CoV-2 propagation and titration

The SARS-CoV-2 isolate SARS-CoV-2 USA/WA/2020 from Microbiologics (Batch number: G2027B) was propagated to generate high-titer virus stocks. Vero E6 (ATCC-CRL1586) cells were used referencing an earlier published protocol (18).

Flow cytometry

Single-cell suspensions from the mouse lungs after collagenase treatment (8 mg/mL) for 1 hour were used for fluorescence-activated cell sorting (FACS) staining. The following antibodies were used: anti-mouse CD4 (BV650, clone RM4-4—BioLegend), CD8a (BV711,

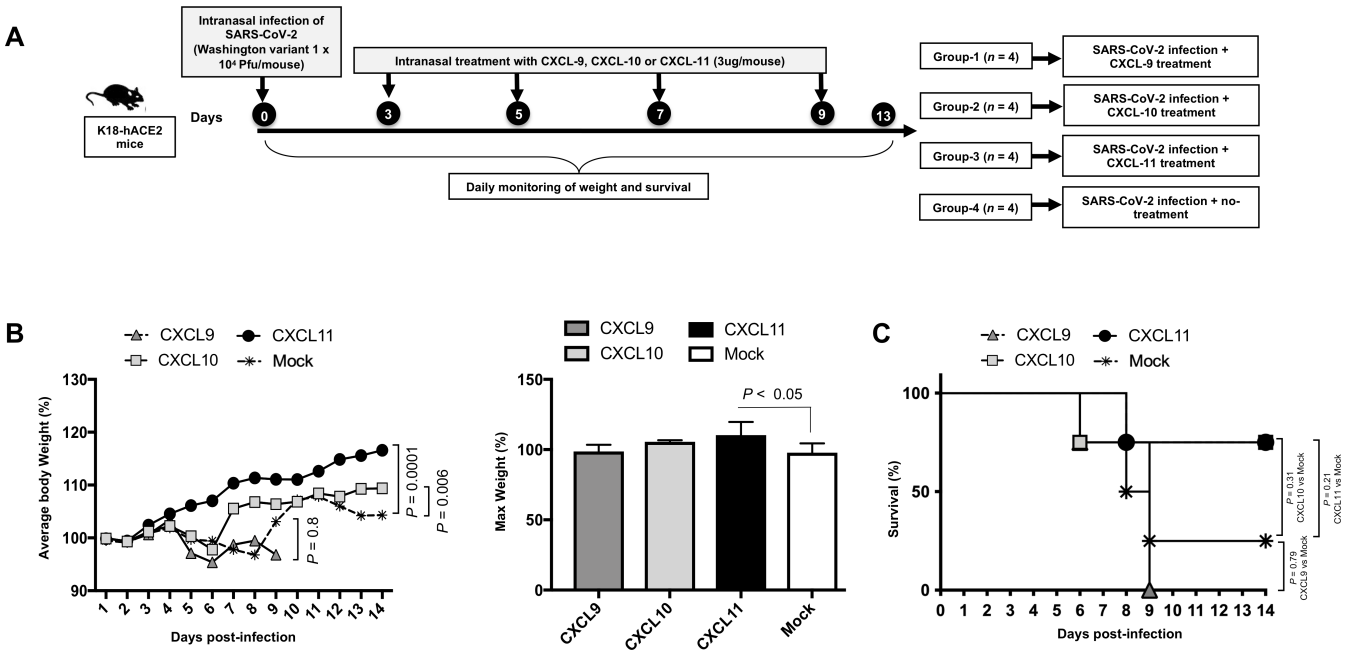

FIG 1 The effect of treatment with CXCL-9, CXCL-10, and CXCL-11 chemokines on COVID-19-like symptoms detected from K18-hACE2 single transgenic mice infected with SARS-CoV-2. (A) Experimental plan to study the effect of treatment with CXCL-9, CXCL-10, and CXCL-11 chemokines on COVID-19-like symptoms detected from K18-hACE2 single transgenic mice following infection with SARS-CoV-2 (Washington USA-WA1/2020 variant). Male and female K18-hACE2 mice (n = 16) 8–9 weeks old were infected intranasally with 1×10^4 pfu of the SARS-CoV-2-USA-WA1/2020 variant. Mice were subsequently treated intranasally with 3 µg of CXCL-9 (n = 4), CXCL-10 (n = 4), and CXCL-11 (n = 4) on days 3, 5, 7, and 9 post-infection, and the control mice (n = 4) were left untreated. (B) Graph shows average body weight change p.i. normalized to the body weight on the day of infection (right panel). The maximum percent body weight change on day 7 p.i. is shown in the left panel. (C) Shows the percentage survival detected in CXCL-9, CXCL-10, and CXCL-11 treated vs untreated mice up to day 13 p.i. The data represent two independent experiments; the graphed values and bars represent the SD between the two experiments.

clone 53-6.7—BioLegend), CD44 (Alexa Fluor 488, clone IM7—BioLegend) , CD62L (Alexa Fluor 700, clone MEL-14—BioLegend) , CD103 (BUV395, clone M290—BD), and CD183 (CXCR3) (PE/Cyanine7, clone CXCR3-173—BioLegend). Surface staining was performed by adding mAbs against various cell markers to 1×10^6 cells in phosphate-buffered saline containing 1% FBS and 0.1% sodium azide and left for 45 minutes at 4°C. Cells were washed three times with FACS buffer and fixed in PBS containing 2% paraformaldehyde (Sigma-Aldrich, St. Louis, MO).

Immunohistochemistry

The HLA-DR*0101/HLA-A*0201/hACE2 triple transgenic mice lung sections were fixed in 4% PFA for 48 hours and then transferred to 70% ethanol. The tissue sections were embedded in paraffin blocks and sectioned at 8 µm thickness. Slides were deparaffinized and rehydrated before hematoxylin and eosin (H&E) staining for routine immunopathology. Furthermore, to compare the relative expression of the SARS-CoV-2 nucleocapsid protein following immunization and various chemokine treatments, immunohistochemistry (IHC) was performed on the lung tissues of HLA-DR*0101/HLA-A*0201/hACE2 triple transgenic mice that were immunized with CoV-Vacc alone, with CoV-Vacc + CXCL9 treatment, with CoV-Vacc + CXCL10 treatment, and with CoV-Vacc + CXCL11 treatment. Images were captured on the BZ-X710 All-in-One Fluorescence Microscope (Keyence).

Virus titration in oropharyngeal swabs

Throat swabs were analyzed for SARS-CoV-2 specific RNA by qRT-PCR. As recommended by the CDC, we used *ORF1ab*-specific primers (forward-5′-CCCTGTGGGTTTTACACTTAA-3′ and reverse-5′-ACGATTGTGCATCAGCTGA-3′) and probe (6FAM-CCGTCTGCGGTATGTGGAA AGGTTATGG-BHQ) to detect the viral RNA level in lungs.

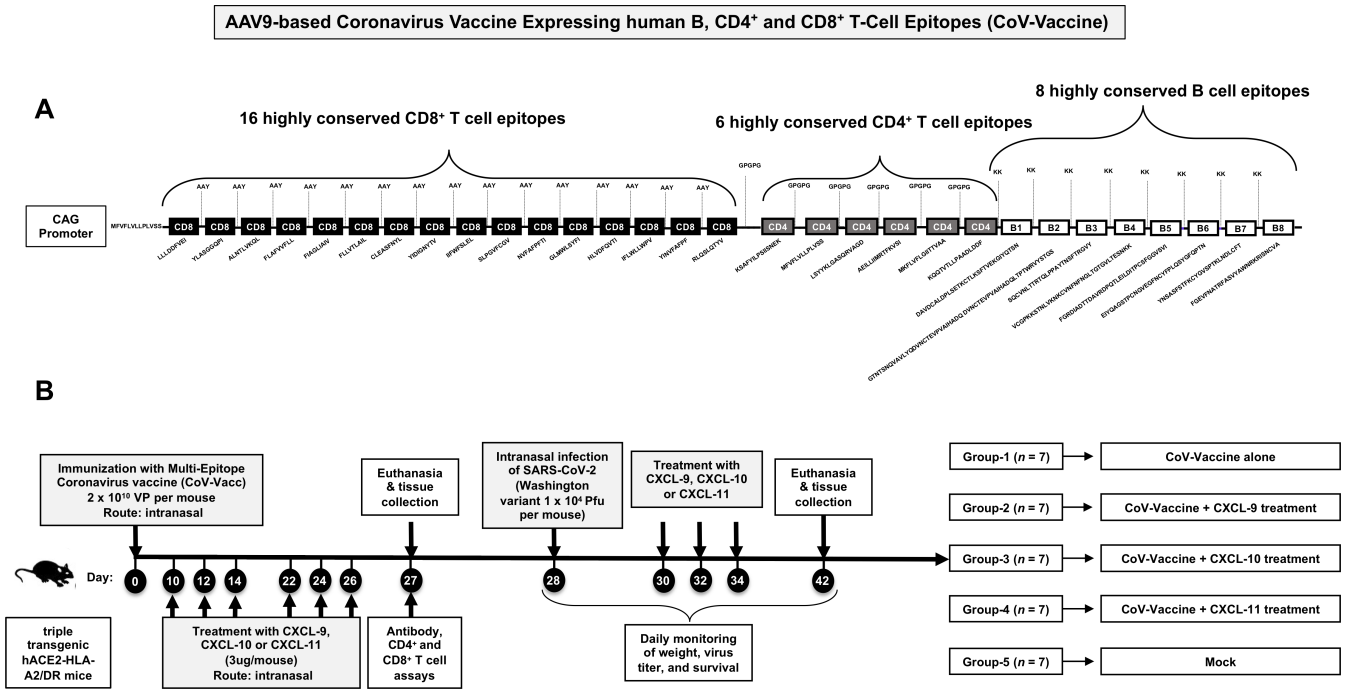

FIG 2 The effect of treatment with CXCL-9, CXCL-10, and CXCL-11 chemokines on disease outcome detected from HLA-DR*0101/HLA-A*0201/hACE2 triple transgenic mice immunized with SARS-CoV-2 vaccine. (A) Figure showing a prototype of the multi-epitope coronavirus vaccine consisting of highly conserved and immunogenic 16 $CD8^+$ T cell epitopes, 6 $CD4^+$ T cell epitopes, and 8 B cell epitopes. (B) Experimental plan to study the effect of treatment with CXCL-9, CXCL-10, and CXCL-11 chemokines on COVID-19-like symptoms detected from HLA-DR*0101/HLA-A*0201/hACE2 triple transgenic mice immunized with multi-epitope coronavirus vaccine. Male and female HLA-DR*0101/HLA-A*0201/hACE2 triple transgenic mice 8–9 weeks old were intranasally immunized with CoV-Vacc; 2×10^{10} VP per mice on day 0 (n = 35). Control mice (n = 7) were left unimmunized. The immunized mice were subsequently treated intranasally with 3 µg of CXCL-9 (n = 7), CXCL-10 (n = 7), and CXCL-11 (n = 7) on days 10, 12, 14, 22, 24, and 26 post-immunization. On day 27 of the experiment, two mice per group were euthanized, and lung tissues were collected. The immune cell response was evaluated by flow cytometry. The remaining mice (n = 25) were intranasally infected with 1×10^4 pfu of SARS-CoV-2 (USA-WA1/2020) on day 28 post-immunization. Three mice groups were subsequently treated intranasally with CXCL-9 (n = 5), CXCL-10 (n = 5), and CXCL-11 (n = 5) on days 30, 32, and 34 post-immunizations. Disease monitoring, weighing, and survival were monitored in the mice up to day 14 p.i. The data represent two independent experiments; the graphed values and bars represent the SD between the two experiments.

Briefly, 5 mL of the total nucleic acid eluate was added to a 20-mL total volume reaction mixture [1× TaqPath 1-Step RT-qPCR Master Mix (Thermo Fisher Scientific, Waltham, MA)], with 0.9 mM each primer and 0.2 mM each probe. The qRT-PCR was carried out using the ABI StepOnePlus thermocycler (Life Technologies, Grand Island, NY). When the Ct-value was relatively high ($35 \leq Ct < 40$), the specimen was retested twice and considered positive if the Ct-value of any retest was less than 35.

Statistical analysis

Data for each assay were compared by ANOVA and Student's t-test using GraphPad Prism version 5 (La Jolla, CA). The physical estimation data were analyzed with the paired t-test using a non-parametric Gaussian distribution based on the Wilcoxon matched-pairs signed-rank test. As previously described, differences between the groups were identified by ANOVA and multiple comparison procedures (14, 16, 19). Data are expressed as the mean + SD. Results were considered statistically significant at $P < 0.05$.

RESULTS

Treatment of SARS-CoV-2-infected K18-hACE2 mice with CXCL-11 T cell-attracting chemokine improves COVID-19-like symptoms and survival

We first tested a dose escalation of 1, 3, and 10 µg of CXCL-9, CXCL-10, and CXCL-11 chemokines, delivered in SARS-CoV-2-infected K18-hACE2 mice (male and female), to

determine the optimal dose of each chemokine that would promote T cell infiltration into the lungs and improve COVID-19-like symptoms. The results identified 3 µg for each chemokine as the optimal dose for enough T cell infiltration into the lungs that was associated with a significant improvement in COVID-19-like symptoms in SARS-CoV-2-infected K18-hACE2 mice (data not shown). Subsequently, 8-week-old female K18-hACE2 transgenic mice (n = 16) were infected intranasally with SARS-CoV-2 (1×10^4 pfu/mouse of Washington USA-WA1/2020 variant) and were left untreated (control) or treated intranasally on days 3, 5, 7, and 9 post-infection with 3 µg of CXCL-9, CXCL-10, or CXCL-11 chemokine (Fig. 1A). Chemokine-treated and untreated mice were then followed daily for morbidity (weight loss) and survival. CXCL-11-treated K18-hACE2 mice showed the best outcomes with significant protection against weight loss (Fig. 1B; Fig. S3) and death (Fig. 1C) compared to the SARS-CoV-2-infected untreated control K18-hACE2 mice (P < 0.05). In contrast, CXCL-9-treated K18-hACE2 mice did not show significant improvement in weight loss (Fig. 1B) and death (Fig. 1C), and CXCL-10-treated K18-hACE2 mice showed modest protection against weight loss (Fig. 1B).

These results support the hypothesis that a prime/pull strategy utilizing chemokines may improve vaccine outcomes.

A multi-epitope/CXCL11 prime/pull coronavirus vaccine protects against COVID-19-like symptoms in HLA-DR*0101/HLA-A*0201/hACE2 triple transgenic mice following infection with SARS-CoV-2

We next determined whether chemokine treatment would improve the protective efficacy of a multi-epitope coronavirus vaccine multiple human B, $CD4^+$, and $CD8^+$ T cell epitopes. For this experiment, we: (i) designed and produced a multi-epitope coronavirus vaccine that co-expresses recently identified 16 highly conserved human $CD8^+$ T cell epitopes, 6 highly conserved human $CD4^+$ T cell epitopes, and 8 highly conserved human B cell epitopes (Table S1), all expressed in tandem under a CMV enhancer/chicken β actin promoter (CAG) in an AAV9 vector (designated as CoV-Vacc, Fig. 2A) and (ii) utilized a novel HLA-DR*0101/HLA-A*0201/hACE2 triple transgenic mice expressing human ACE2, human HLA class 1 (HLA-A*0201), and class 2 (HLA-DR*0101).

As illustrated in Fig. 2A, the prime/pull coronavirus vaccination consists of (i), first, priming of SARS-CoV-2-specific B cells, $CD4^+$ T cells, and $CD8^+$ T cells in HLA-DR*0101/HLA-A*0201/hACE2 triple transgenic mice using the engineered lung-tropic AAV9 multi-epitope coronavirus vaccine co-expressing the recently identified immunodominant B, $CD4^+$, and $CD8^+$ T cell epitopes (i.e., CoV-Vacc) and delivered intranasally followed by (ii) pulling the "primed" B cells, $CD4^+$ T cells, and $CD8^+$ T cells into the lungs using mouse CXCL-9, CXCL-10, or CXCL-11 T cell-attracting chemokines delivered intranasally.

As shown in Fig. 2B, HLA-DR*0101/HLA-A*0201/hACE2 triple transgenic mice (8–9-week old, n = 35) were intranasally immunized with 2×10^{10} VP per mouse of CoV-Vacc. The immunized mice were then divided into five groups of seven mice each and either left untreated with any chemokine (n = 7), or subsequently treated intranasally with 3 µg of CXCL-9 (n = 7), CXCL-10 (n = 7), or CXCL-11 (n = 7) on days 10, 12, 14, 22, 24, and 26 post-immunization. The fifth control group of mice (n = 7) was neither immunized with the CoV-Vacc nor treated with the chemokines (mock).

On day 28 post-immunization, mice were intranasally challenged with 1×10^4 pfu of SARS-CoV-2 (USA-WA1/2020). Subsequently, all vaccinated groups received additional treatment with CXCL-9, CXCL-10, or CXCL-11 on days 30, 32, and 34 post-immunization. All animals were then monitored for up to day 14 p.i. for weight loss, virus replication in the lungs, and death. On day 14 p.i., mice were euthanized, and lungs were collected for lung inflammation with H&E staining.

We observed significant protection against weight loss in the group of mice that received the multi-epitope/CXCL11 prime/pull CoV-Vacc compared to the multi-epitope/CXCL9 prime/pull CoV-Vacc group, the multi-epitope/CXCL10 prime/pull CoV-Vacc group, and the mock control group (P < 0.005, Fig. 3A; Fig. S3). Between days 5 and 9 post-challenge with SARS-CoV-2, the multi-epitope/CXCL11 prime/pull CoV-Vacc

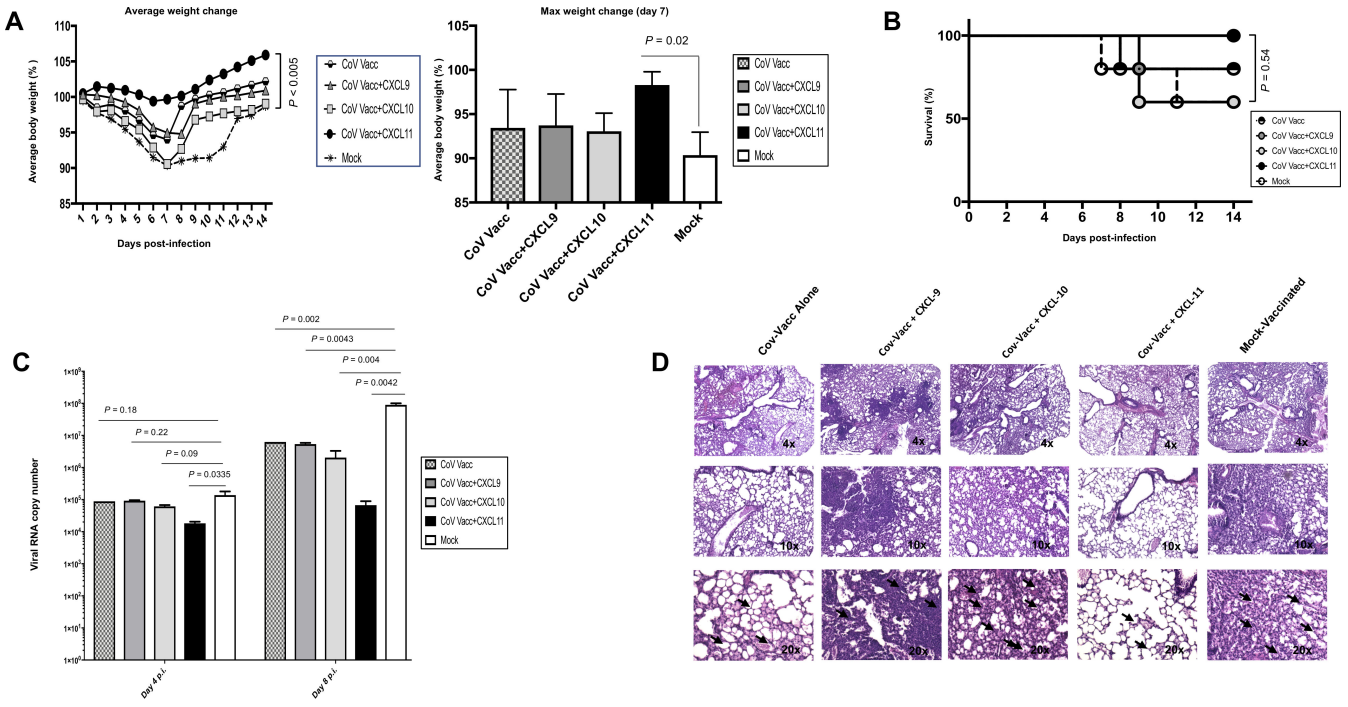

FIG 3 The effect of treatment with CXCL-9, CXCL-10, and CXCL-11 chemokines on COVID-19-like symptoms detected from HLA-DR*0101/HLA-A*0201/hACE2 triple transgenic mice immunized with multi-epitope coronavirus vaccine and challenged with SARS-CoV-2-USA-WA1/2020 variant. (A) Data showing average percent weight change each day p.i. normalized to the body weight on the day of infection are shown in the right panel. The bar graph (left panel) shows the percent weight change at day 7 p.i. Bars represent mean ± SEM. (B) Shows the percentage survival detected in mice groups of CoV-Vacc, CoV-Vacc + CXCL-9, CoV-Vacc + CXCL-10, CoV-Vacc + CXCL-11, and mock-vaccinated group up to 14 days p.i. (C) Viral titration data showing viral RNA copy number in the lungs for each group at days 4 and 8 p.i. (D) Representative H&E staining images of the lungs at day 14 p.i. of SARS-CoV-2-infected mice treated with different chemokines at 4×, 10×, and 40× magnifications. The data represent two independent experiments; the graphed values and bars represent the SD between the two experiments.

group lost only ~2% of their initial weight, whereas the remaining groups showed a significant loss in their initial weight that varied between 4% and 10% (Fig. 3A). Accordingly, a significant reduction in virus replication was recorded in the lungs of multi-epitope/CXCL11 prime/pull CoV-Vacc group of mice compared to other groups (Fig. 3C). Significantly lower viral RNA copy numbers were detected on both days 4 and 8 post-infection in the lungs of the multi-epitope/CXCL11 prime/pull CoV-Vacc group compared to other groups (Fig. 3C). Moreover, from day 0 to day 14 post-challenge with SARS-CoV-2, the multi-epitope/CXCL11 prime/pull CoV-Vacc group of mice showed 100% survival, whereas the remaining groups had only 60% to 80% survival (Fig. 3B). The lowest virus replication was observed in the lungs of multi-epitope/CXCL11 prime/pull CoV-Vacc-treated mice, which was associated with fewer inflammatory cells infiltrating the lungs and lower levels of pulmonary pathological changes characterized by (i) open alveolar air spaces, (ii) less inflammation, and (iii) less residual cellular debris in air spaces with less alveolar damage observed in the H&E sections (Fig. 3D).

These results demonstrate that the multi-epitope/CXCL11 prime/pull strategy enhanced vaccine efficacy against COVID-19-like symptoms, reduced virus replication and inflammation in the lungs, and prevented deaths in HLA-DR*0101/HLA-A*0201/hACE2 triple transgenic mice following infection with SARS-CoV-2. As was observed with the chemokine treatment only, CXCL9 and CXCL10 were not effective.

Increasing the frequencies of lung-resident memory CD4$^+$ and CD8$^+$ T_{EM}, T_{CM}, and T_{RM} cells by the multi-epitope/CXCL11 prime/pull coronavirus vaccine approach

Since the multi-epitope/CXCL11 prime/pull coronavirus vaccine enhanced protection as measured by reduced weight loss, virus replication, inflammation in the lungs, and deaths in HLA-DR*0101/HLA-A*0201/hACE2 triple transgenic mice following infection with SARS-CoV-2, we sought to determine whether this protection was associated with increased frequencies of lung-resident memory CD4$^+$ and CD8$^+$ T cells.

We compared the effect of immunization with the three multi-epitope prime/pull coronavirus vaccine candidates based on CXCL-9, CXCL-10, and CXCL-11 T cell-attracting chemokines on the frequencies of three major lung-resident memory CD4$^+$ and CD8$^+$ T cell subsets [i.e., effector memory (T_{EM}), resident memory (T_{RM}), and central memory (T_{CM})] in the lungs of HLA-DR*0101/HLA-A*0201/hACE2 triple transgenic mice, before (Fig. 4 and 5) challenge with SARS-CoV-2 (Fig. 2B). For controls, the frequencies of three major lung-resident memory CD4$^+$ and CD8$^+$ T cell subsets were compared in HLA-DR*0101/HLA-A*0201/hACE2 triple transgenic mice that received the same multi-epitope CoV-Vacc-bearing human CD4$^+$ and CD8$^+$ T cell epitopes without chemokine treatment (CoV-Vacc alone) as well as in mock-vaccinated mice (mock).

For this experiment, 8–9-week-old HLA-DR*0101/HLA-A*0201/hACE2 triple transgenic mice (n = 35) were first immunized with the multi-epitope coronavirus vaccine delivered intranasally at 2 × 10^{10} VP per mouse. Vaccinated HLA-DR*0101/HLA-A*0201/hACE2 triple transgenic were subsequently left untreated (control) or treated intranasally on days 10, 12, and 14 post-vaccination and on days 22, 24, and 26 post-vaccinations with the CXCL-9, CXCL-10, or CXCL-11 T cell-attracting chemokine as described in

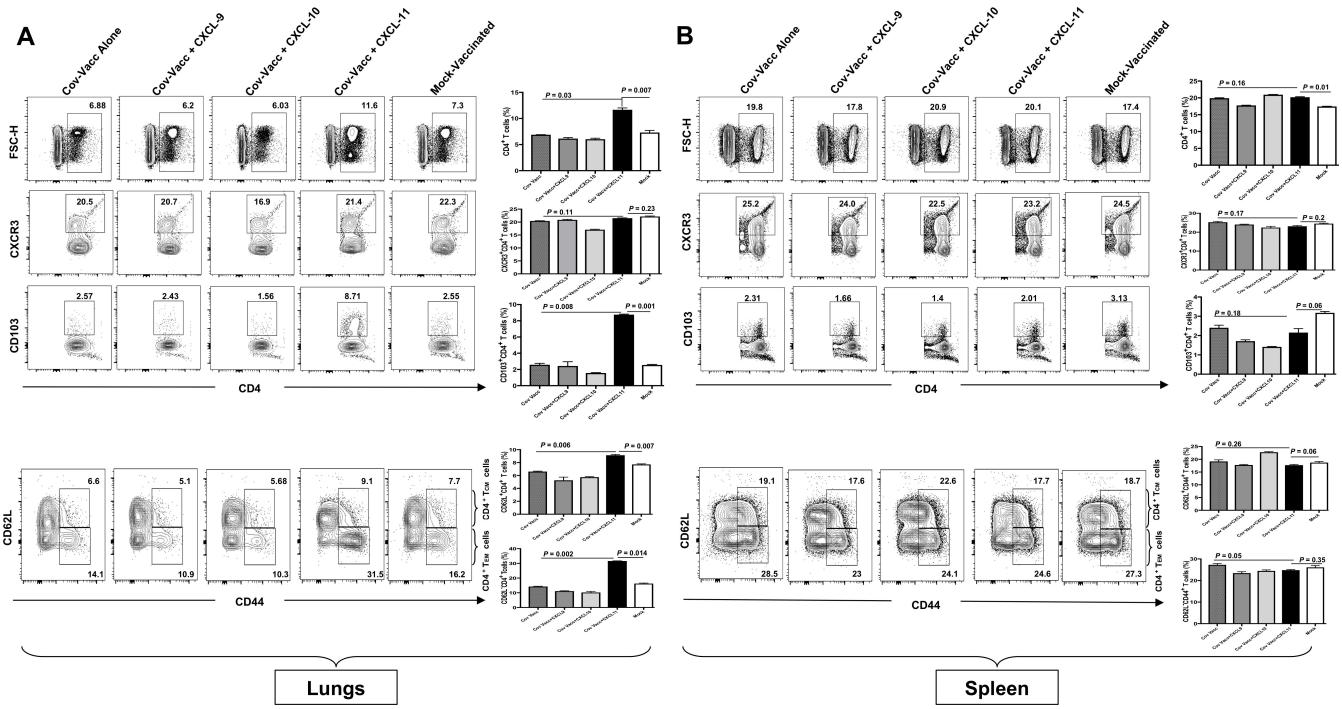

FIG 4 The effect of treatment with CXCL-9, CXCL-10, and CXCL-11 chemokines on CD4$^+$ T cells in the lung and spleen of immunized HLA-DR*0101/HLA-A*0201/hACE2 triple transgenic mice. (A) The left panel shows FACS plots for CD4$^+$ T cells in the lungs of mice immunized with the multi-epitope coronavirus vaccine and treated with CXCL-9, CXCL-10, and CXCL-11. Graphs depict the differences in response to various treatments on the percentage of CD4$^+$ T cells present in the lungs of mice shown in the right panel. Bars represent the mean ± SEM. ANOVA test was used to analyze the data. (B) The left panel represents FACS plots for CD4$^+$ T cells in the spleen of mice immunized with the multi-epitope coronavirus vaccine and treated with CXCL-9, CXCL-10, and CXCL-11. Graphs on the right panel show the difference in response to different chemokine treatments on the percentage of CD4$^+$ T cells in the spleen of mice. The data represent two independent experiments; the graphed values and bars represent the SD between the two experiments.

Materials and Methods. Vaccinated/chemokine-treated and vaccinated/untreated mice were euthanized on day 27 post-vaccination, and the frequencies of the three major lung-resident memory $CD4^+$ and $CD8^+$ T cells expressing CXCR3, CD103, CD62L, and CD44 among total lung cells [i.e., effector memory (T_{EM}), resident memory (T_{RM}), and central memory (T_{CM})] were determined by FACS, as described in Materials and Methods.

A significant increase was observed in the frequency of total $CD4^+$ T cells among immunized mice compared to mock mice (Fig. 4A). Similarly, we found a significant increase in $CD103^+CD4^+$ T cells, $CD44^+CD62L^-CD4^+$ T cells, and $CD44^+CD62L^+CD4^+$ T cells in mice immunized with the CoV-Vacc. However, $CXCR3^+CD4^+$ T cells did not show significant variation for mice immunized with CoV Vacc + CXCL-9, CoV Vacc + CXCL-10, or CoV Vacc + CXCL-11 compared to mice immunized only with Vacc or mock group of mice. In Fig. 5A, a higher magnitude in the frequency of total $CD8^+$ T cells in lung immune cells was observed in the immunized mice. Furthermore, the mice immunized with CoV Vacc showed a significant increase in $CXCR3^+CD8^+$ T cells, $CD44^+CD62L^-CD8^+$ T cells, and $CD44^+CD62L^+CD8^+$ T cells when compared to the mock group. However, $CD103^+CD8^+$ T cells showed a decrease in the CoV Vacc + CXCL-11 group compared to the immunized and mock groups. As shown in Fig. 4B and 5B; Fig. S1, no significant difference was observed in the frequencies of $CD4^+$ and $CD8^+$ T cells among immunized and chemokine-treated mice compared to CoV Vacc and mock mice in the spleens.

These results demonstrate that the protection induced by the multi-epitope/CXCL11 prime/pull coronavirus vaccine in SARS-CoV-2-infected HLA-DR*0101/HLA-A*0201/hACE2 triple transgenic mice is associated with high frequencies of lung-resident memory $CD4^+$ and $CD8^+$ T_{EM}, T_{CM}, and T_{RM} cells.

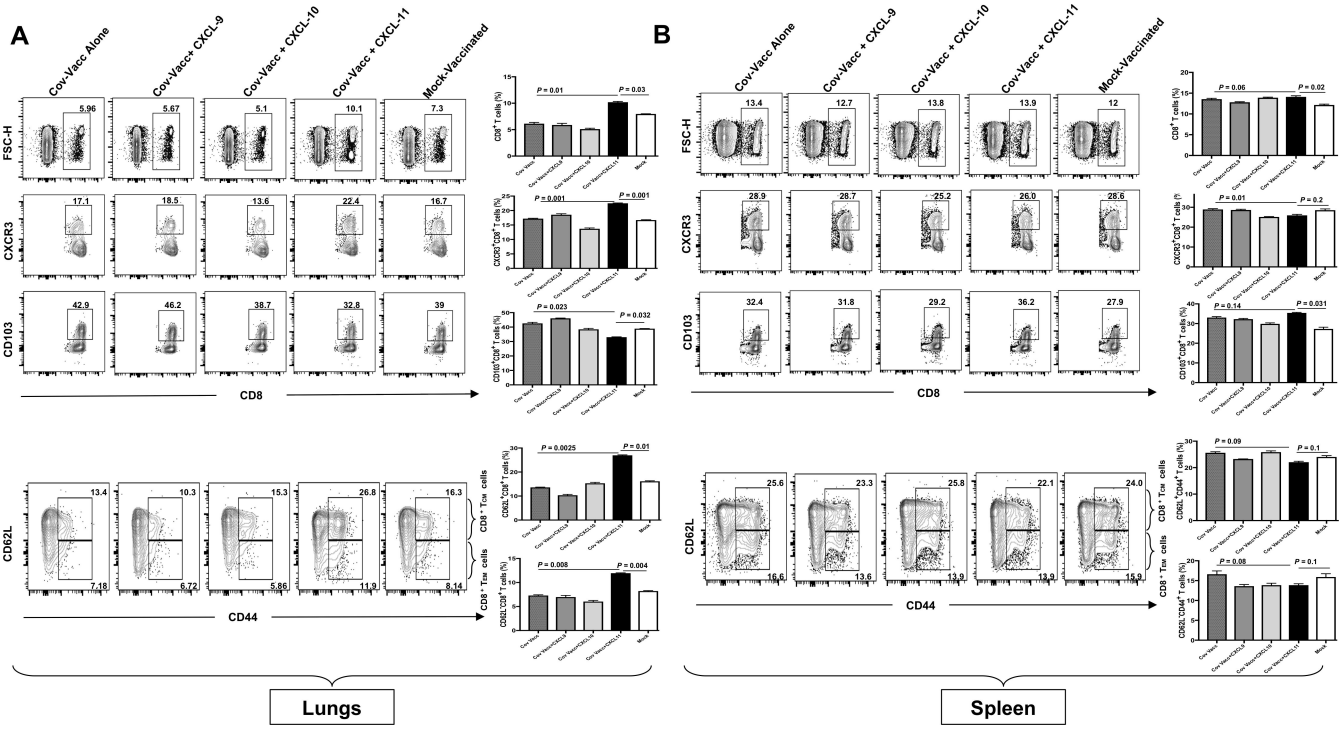

FIG 5 The effect of treatment with CXCL-9, CXCL-10, and CXCL-11chemokines on $CD8^+$ T cells in the lung and spleen of immunized HLA-DR*0101/HLA-A*0201/hACE2 triple transgenic mice. (A) The left panel shows FACS plots for $CD8^+$ T cells in the lungs of mice immunized with the multi-epitope coronavirus vaccine and treated with CXCL-9, CXCL-10, and CXCL-11. Graphs depict the differences in response to various treatments on the percentage of $CD8^+$ T cells present in the lungs of mice shown in the right panel. Bars represent the mean ± SEM. ANOVA test was used to analyze the data. (B) The left panel represents FACS plots for $CD8^+$ T cells in the spleen of mice immunized with the multi-epitope coronavirus vaccine and treated with CXCL-9, CXCL-10, and CXCL-11. Graphs on the right panel show the difference in response to different chemokine treatments on the percentage of $CD4^+$ T cells in the spleen of mice. The data represent two independent experiments; the graphed values and bars represent the SD between the two experiments.

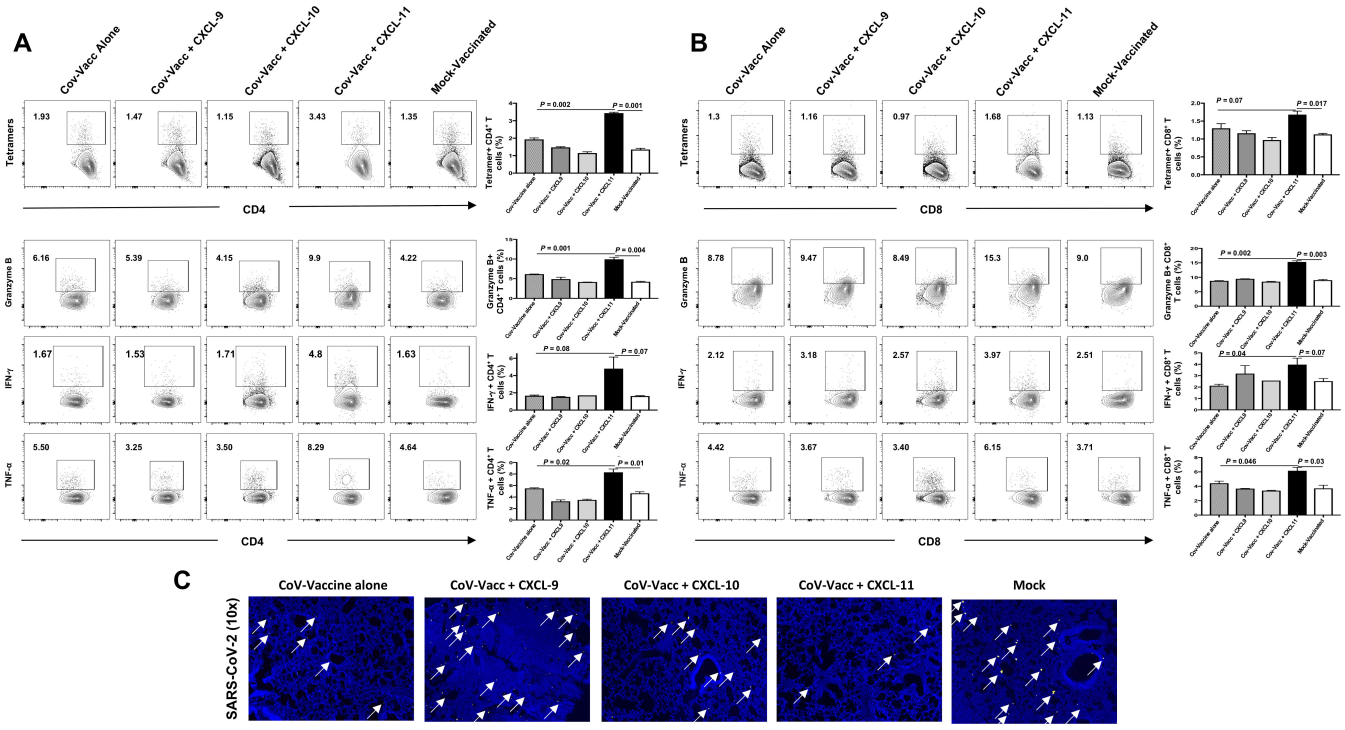

FIG 6 The effect of treatment with CXCL-9, CXCL-10, and CXCL-11 chemokines on $CD4^+$ T cells and $CD8^+$ T cells in the lung of immunized HLA-DR*0101/HLA-A*0201/hACE2 triple transgenic mice. (A) The left panel shows FACS plots for $CD4^+$ T cells, using a pool of tetramers representing the $CD4^+$ T cell in the vaccine, in the lungs of mice immunized with the multi-epitope coronavirus vaccine and treated with CXCL-9, CXCL-10, and CXCL-11. Graphs depict the differences in response to various treatments on the percentage of $CD4^+$ T cells present in the lungs of mice shown in the right panel. Bars represent the mean ± SEM. ANOVA test was used to analyze the data. (B) The left panel represents FACS plots for $CD8^+$ T cells, using a pool of tetramers representing the $CD8^+$ T cell in the vaccine, in the lungs of mice immunized with the multi-epitope coronavirus vaccine and treated with CXCL-9, CXCL-10, and CXCL-11. Graphs on the right panel show the difference in response to different chemokine treatments on the percentage of $CD8^+$ T cells in the lungs of mice. (C) Representative IHC sections of triple transgenic hACE2-HLA-A2/DR mice lung tissue collected 14 days after exposure to SARS-CoV-2, stained with SARS-CoV-2 nucleocapsid antibody in yellow, arrows indicate virus staining. The data represent two independent experiments; the graphed values and bars represent the SD between the two experiments.

Increasing the function of virus-specific lung-resident memory $CD4^+$ and $CD8^+$ T cells by the multi-epitope/CXCL11 prime/pull coronavirus vaccine approach

Since the protection induced by the multi-epitope/CXCL11 prime/pull coronavirus vaccine in SARS-CoV-2-infected HLA-DR*0101/HLA-A*0201/hACE2 triple transgenic mice is associated with higher frequencies of lung-resident memory $CD4^+$ and $CD8^+$ T_{EM}, T_{CM}, and T_{RM} cells, we next determined whether such protection was associated with the increased functionality of lung-resident memory $CD4^+$ and $CD8^+$ T cells. We compared the effect of immunization with the three multi-epitope prime/pull coronavirus vaccine candidates based on CXCL-9, CXCL-10, and CXCL-11 T cell-attracting chemokines before challenging with SARS-CoV-2 (Fig. 6). As controls, we used (i) HLA-DR*0101/HLA-A*0201/hACE2 triple transgenic mice, which received the same multi-epitope CoV-Vacc bearing human $CD4^+$ and $CD8^+$ T cell epitopes without chemokine treatment (CoV Vacc alone), and (ii) mock-vaccinated mice (mock) which were not vaccinated with CoV-Vacc or treated with the chemokines.

For this experiment, 8–9-week-old HLA-DR*0101/HLA-A*0201/hACE2 triple transgenic mice (n = 35) were first immunized with the multi-epitope coronavirus vaccine (CoV-Vacc) delivered intranasally at 2×10^{10} VP per mouse. Vaccinated HLA-DR*0101/HLA-A*0201/hACE2 triple transgenic mice were subsequently left untreated (control) or treated intranasally on days 10, 12, and 14 post-vaccination and on days 22, 24, and

26 post-vaccination with the CXCL-9, CXCL-10, or CXCL-11 T cell-attracting chemokine as described in Materials and Methods. Vaccinated/chemokine-treated and vaccinated/untreated mice were euthanized on day 27 post-vaccination, and immune cells were harvested for the frequency and the function of major lung memory $CD4^+$ and $CD8^+$ T cells determined by FACS, as described in Materials and Methods.

We found a significant increase in the percentage of tetramer$^+$ $CD4^+$ T cells (pool of tetramers representing the $CD4^+$ T cell in the vaccine) among immunized and CXCL11-treated mice compared to all other mice groups (Fig. 6A). Similarly, we found a significant increase in Granzyme B^+ $CD4^+$ T cells, IFN-γ^+CD4^+ T cells, and TNF-α^+CD4^+ T cells in mice immunized with the CoV-Vacc and treated with the chemokine CXCL11 but not with CXCL9 or CXCL10. Similarly, an increase in magnitude in the percentage of tetramer$^+$ $CD8^+$ T cells (pool of tetramers representing the $CD8^+$ T cell in the vaccine) was seen in the lungs of immunized and CXCL11-treated mice compared to all other mice groups (Fig. 6B). Significant increases in Granzyme B^+ $CD8^+$ T cells and TNF-α^+CD8^+ T cells were also observed in the lungs of the CoV Vacc + CXCL-11 group compared to the immunized and mock groups. IFN-γ^+CD8^+ T cells were not significantly increased among all the groups. No significant differences in spike-specific antibody titers were detected in animals that received the CoV-Vacc alone compared to animals that received CoV-Vacc together with treatment with CXCL11, CXCL9, or CXCL10 chemokines (Fig. S2).

We performed nucleocapsid-specific antibody-based IHC staining on lung tissues from vaccinated/treated and unvaccinated/untreated HLA-DR*0101/HLA-A*0201/hACE2 triple transgenic mice. As shown in Fig. 6C, we observed a significant reduction in the expression of SARS-CoV-2 nucleocapsid protein in the lungs of CoV-vaccinated and CXCL11 treatment compared to the lungs of unvaccinated and untreated mice (Fig. 6C). In addition, a gradual reduction in the expression of SARS-CoV-2 nucleocapsid protein was observed in the lungs of the CoV-Vacc + CXCL11-treated group followed by CoV-Vacc alone, CoV-Vacc + CXCL10, CoV-Vacc + CXCL9, and mock groups (Fig. 6C).

Taken together, these results demonstrate that the protection induced by the multi-epitope/CXCL11 prime/pull coronavirus vaccine in SARS-CoV-2-infected HLA-DR*0101/HLA-A*0201/hACE2 triple transgenic mice is associated with high frequencies of virus-specific functional $CD4^+$ and $CD8^+$ T cells in the lungs, expressing Granzyme B and producing both IFN-γ and TNF-α.

DISCUSSION

Over 3 years have passed since humanity was confronted by COVID-19 (20). Parenteral COVID-19 vaccines have induced neutralizing antibodies against COVID-19, but they have failed to induce SARS-CoV-2-specific memory $CD4^+$ and $CD8^+$ T cells in the lungs (21). It has been shown that parenteral vaccines are less effective in inducing mucosal T cell immunity than mucosal vaccines (13). These low frequencies of memory SARS-CoV-2-specific $CD4^+$ and $CD8^+$ T cells in the lungs are associated with severe cases of acute and long-term COVID-19, even in some vaccinated patients (22). In addition, because many mutations and deletions in the six SARS-CoV-2 variants (Wuhan, Alpha, Beta, Gamma, Delta, and Omicron) occur within the Spike protein gene, there is a risk that current Spike-based COVID-19 subunit vaccines will not protect against future variants of concern (VOCs), despite generating strong neutralizing antibodies against the original virus strain (23). This underscores the need for next-generation coronavirus vaccines that (i) target antigens (Ags) other than the highly variable Spike protein, (ii) incorporate both B and T cell epitopes from Spike and non-Spike Ags that are highly conserved across all VOCs to stimulate strong cross-strain humoral and cell-mediated immunity, and (iii) can increase SARS-CoV-2-specific $CD4^+$ and $CD8^+$ T cells in the lungs.

The current parenteral subunit COVID-19 vaccines that rely primarily on neutralizing Spike-specific antibodies have substantially prevented SARS-CoV-2-related hospital admissions and deaths. However, Spike-alone-based vaccines have induced low frequencies of memory SARS-CoV-2-specific $CD4^+$ and $CD8^+$ T cells in the lungs that are associated with severe cases of acute and long COVID-19, even in some boosted

patients (24). To address this limitation, we utilized a novel multi-epitope/CXCL11 prime/pull coronavirus mucosal vaccine strategy to boost the frequencies of functional $CD4^+$ and $CD8^+$ T_{EM}, T_{CM}, and T_{RM} cells in the lungs of HLA-DR*0101/HLA-A*0201/hACE2 triple transgenic mice leading to enhanced protection against SARS-CoV-2 infection, COVID-19-like symptoms, and death. This highlights the importance of lung-resident $CD4^+$ and $CD8^+$ memory T cells in protection against SARS-CoV-2 infection, COVID-19-like symptoms, and death (24). Moreover, T cell-based vaccines are critical in SARS-CoV-2 as they can provide long-lasting memory immunity that could potentially protect against repetitive infection with multiple variants. $CD4^+$ and $CD8^+$ memory T cells can recognize and eliminate infected cells and provide memory immunity in case of re-exposure (6). In addition, unlike antibody-based vaccines, T cell-based vaccines have greater potential to protect against new and mutated strains of the virus (25).

Chemokines play a complex role in the immune response to viral infections, including SARS-CoV-2, by stimulating the production of antiviral proteins, such as interferons. However, excessive or dysregulated production of certain chemokines may contribute to the development of severe COVID-19 (26). Chemokines are important targets for the development of therapeutics to treat different infectious diseases, including SARS-CoV-2; however, the explicit roles of these chemokines in SARS-CoV-2 immunity remain to be fully explored. Coperchini et al. have screened for the immune responses that involve cytokine activation; these chemokines are affiliated with immune cell trafficking, respiratory infection regulation, and the chemoattraction of T cells (27). The prime-pull approach has been used experimentally with several vaccine targets, including influenza, HPV, and hepatitis B (28).

Following acute infection, three major SARS-CoV-2-specific memory $CD4^+$ and $CD8^+$ T cell sub-populations, T_{CM}, T_{EM}, and T_{RM}, develop, infiltrate, and sequester in the infected lungs in response to a high level of T cell-attracting CXCL9, CXCL10, and CXCL11 chemokines and other factors. Memory $CD4^+$ and $CD8^+$ T cell infiltrates have been reported in the infected lungs of COVID-19 human cadavers (29). Functional $CD4^+$ and $CD8^+$ T cells in these infiltrates likely help decrease viral replication in the lungs, the brain, and possibly other compartments. However, the low levels of the T cell-attracting CXCL9, CXCL10, and CXCL11 chemokines in infected lungs may not be sufficient to facilitate the sequestration of $CD4^+$ and $CD8^+$ T_{RM} cells or to guide homing $CD4^+$ and $CD8^+$ T_{EM} and T_{CM} cells from circulation into infected lungs. In this study, we found that local delivery of the T cell-attracting CXCL11 chemokine, but not of CXCL9 or CXCL10 chemokines, markedly increased both the number and function of SARS-CoV-2-specific $CD4^+$ and $CD8^+$ T_{EM} and T_{RM} cell sub-populations in infected lungs, thereby improving protection against virus replication, COVID-19-like symptoms, and death in SARS-CoV-2-infected HLA-DR*0101/HLA-A*0201/hACE2 triple transgenic mice. These results suggest that (i) the number and the function of $CD4^+$ and $CD8^+$ T cells specific for "ASYMP" epitopes may be suppressed in the lungs of COVID-19 patients; (ii) local delivery of the T cell-attracting CXCL11 chemokine will expand the repertoire and function of SARS-CoV-2-specific $CD8^+$ T cells and reduce the likelihood of viral replication in the lungs; and (iii) a prime/pull vaccine strategy that increases the number and function of $CD4^+$ and $CD8^+$ T cells in infected lungs over a certain threshold would likely lead to enhanced protection in humans. The success of this innovative prime/pull vaccine may be due to the expansion and survival characteristics of $CD4^+$ and $CD8^+$ T cell precursors, as well as an increase in the number and function of other immune cells in lungs, including APCs following CXCL11 treatment (19). This contributes not only to the homing of $CD4^+$ and $CD8^+$ T_{EM} cell sub-populations in infected lungs but also to the increased expansion and survival of local tissue-resident $CD4^+$ and $CD8^+$ T_{RM} cells that were already present within the lungs.

SARS-CoV-specific $CD4^+$ and $CD8^+$ T cells that reside in the lungs appeared to play a critical role in aborting virus replication (30). In designing an effective human multi-epitope coronavirus vaccine, it is critical to identify the protective coronavirus epitopes contained within the open reading frames (ORFs) of the SARS-CoV-2 genome. Such epitopes are preferentially recognized by the human $CD4^+$ and $CD8^+$ T cells from

"naturally" protected ASYMP individuals who, despite being infected, do not develop COVID-19 disease (31). We previously implemented several *in silico, ex vivo*, *in vitro*, and *in vivo* phenotypic and functional immunological methods to efficiently generate a genome-wide map of the responsiveness of SARS-CoV-2-specific $CD4^+$ and $CD8^+$ T cells in ASYMP individuals, leading to the identification of several previously unknown protective human "ASYMP" $CD4^+$ and $CD8^+$ T cell epitopes. These "ASYMP" epitopes are associated with frequent, robust, and polyfunctional $CD4^+$ and $CD8^+$ T_{EM} cell responses. The present study extends these previous findings by demonstrating that immunization of a novel "humanized" susceptible HLA-DR*0101/HLA-A*0201/hACE2 triple transgenic mouse model with these "ASYMP" epitopes induced a strong $CD4^+$ and $CD8^+$ T cell-dependent protective immunity against COVID-19-like symptoms. Furthermore, utilizing the novel prime-pull vaccine strategy, based on priming $CD4^+$ and $CD8^+$ T cells with multiple "ASYMP" epitopes followed by treatment with the CXCL11 T cell-attracting chemokine, significantly boosted the number of functional anti-viral $CD4^+$ and $CD8^+$ T_{EM} and T_{RM} cells in the lungs of SARS-CoV-2-infected mice and improved protection against COVID-19-like symptoms. These findings have important implications for the development of T cell-based prophylactic COVID-19 vaccine strategies to protect against COVID-19 infections and diseases in humans.

In the era of omics, multiple B and T cell epitope-based vaccines are being developed to tackle other coronavirus infections and diseases for which vaccine development has been unsuccessful (32). However, low frequencies of SARS-CoV-2-specific $CD4^+$ and $CD8^+$ T cells have hampered genome-wide identification of protective SARS-CoV-2 $CD4^+$ and $CD8^+$ T cell epitopes that are associated with the "natural protective immunity" seen in asymptomatic COVID-19 patients (21). The recent availability of comprehensive genomic data sets of SARS-CoV-2 has shifted the paradigm of vaccine development from virological to sequence-based approaches (33). Our recent genome-wide screening of the SARS-CoV-2 sequence using cohorts of symptomatic (SYMP) and asymptomatic (ASYMP) COVID-19 patients identified several previously unknown $CD4^+$ and $CD8^+$ T cell epitopes that span a wide range of structural and non-structural SARS-CoV-2 proteins (14, 15, 19). Previously, we characterized the phenotype and function of $CD4^+$ and $CD8^+$ T cell epitopes in ASYMP COVID-19 patients and "humanized" HLA-DR*0101/HLA-A*0201 double transgenic mice (14). The present study extended our previous report and implemented an innovative prime/pull vaccine strategy that increases the size and function of SARS-CoV-2-specific $CD4^+$ and $CD8^+$ T cells in infected lungs. Our study demonstrated for the first time a protective efficacy against SARS-CoV-2 infection, COVID-19-like symptoms, and death in a "humanized" HLA-DR*0101/HLA-A*0201/hACE2 triple transgenic mouse model (15).

The inadequacy of many animal models of SARS-CoV-2 infection and immunity has made it challenging to explore the immune mechanisms that lead to protection against COVID-19 (34). One critical question is which animal model would be the most appropriate to mimic the immuno-pathological aspects of COVID-19 symptoms as occur in humans? ACE-2 transgenic mice have been the animal models of choice for most COVID-19 immunologists, and the results from ACE-2 transgenic mouse model have yielded substantial insights into the protective mechanisms during primary acute infection (35, 36). Characterization of the phenotype and function of protective SARS-CoV-2-specific memory $CD4^+$ and $CD8^+$ T cells in ACE-2 transgenic mice has been largely limited to T cells specific to the immunodominant SARS-CoV-2 mouse epitopes studied during acute infection (37, 38). In the present study, we used a novel "humanized" susceptible HLA-DR*0101/HLA-A*0201/hACE2 triple transgenic mouse model and validated it for COVID-19 disease. We evaluated its safety, immunogenicity, and protective efficacy in the context of our multi-epitope/CXCL11 prime/pull coronavirus mucosal vaccine. Importantly, these triple transgenic mice express the human HLA-A*0201 and HLA-DR*0101-molecules, in place of mouse MHC molecules. Hence, this introduces an important new small animal model to study the role of HLA-restricted

$CD4^+$ and $CD8^+$ T cells specific to human SARS-CoV-2 epitopes in protection against virus replication and COVID-19-like symptoms.

In the present study, for most experiments, we chose the oropharyngeal swab (over lung tissues) because of multiple practical and safety considerations: (i) collection of oropharyngeal swab samples can be performed at multiple time points without having to euthanize the animals. In contrast, collecting lung tissue to perform viral titration requires the euthanasia of animals at each time point, which would result in a substantial increase in the number of animals to be enrolled in each experiment. Because of the limitation of animals on our HLA-DR*0101/HLA-A*0201/hACE2 triple transgenic mouse colony, we could not use large numbers of animals in this colony at multiple time points to collect the lungs and perform viral titration; and (2) practical and safety restrictions limit the ability to perform multiple time point experiments in the high-containment BSL3 laboratory. Thus, we adapted the approach of collecting nasopharyngeal swabs in our mouse models infected with the SARS-CoV-2 WA/USA variant.

In this present study, we chose the qPCR-based approach for viral titration (over the plaque assay) because of practical and safety considerations: (i) the CDC recommendation that nasopharyngeal and oropharyngeal swabs are good sources to measure SARS-CoV-2 viral titer in humans (39); and (ii) although the plaque assay is considered one of the gold standards of viral titration, the qPCR also offers several advantages, such as a lower threshold of detection; the potential stability of the assay after specimen freezing and thawing, thus permitting sample batching; a less subjective assay readout; and an assay that is unaffected by therapeutic passive neutralizing antibodies or experimental antiviral agents. On day 14 p.i., at the end of experiments, we euthanized the HLA-DR*0101/HLA-A*0201/hACE2 triple transgenic and K18-hACE2 mice, and the lungs were collected for viral titration.

The lung-tropic AAV9 vector used in our prime/pull vaccine has rapidly moved to the forefront of human therapies in the past few years (40). We chose AAV9 because (i) it is a lung-tropic virus with the potential of persistent transgene expression in epithelial cells; (ii) it can superinfect SARS-CoV-2-infected cells; (iii) it can accommodate insertion of up to 4.7 kb of DNA; and (iv) it is non-pathogenic. Clinical trials using AAV vectors have shown only transient inflammation while demonstrating clinical benefits. No side effects were observed in SARS-CoV-2-infected mice during the 30 days of monitoring following treatment with the AAV9 vector. However, long-term monitoring of the lungs and brain for pathology associated with AAV9 will be necessary to ensure the vectors' safety for eventual use in COVID-19 patients. A novelty of this study is to evaluate the safety and protective efficacy of the multi-epitope coronavirus vaccine in a triple transgenic HLA-DR*0101/HLA-A*0201/hACE2 mice model. The experiment is meant to "priming" T cells with the CoV-Vacc comprising $CD8^+$ T cell and $CD4^+$ T cell epitopes and "pulling" the primed T cells into infected lung tissues by administering T cell-attracting chemokines: CXCL9, CXCL10, or CXCL11. These T cell-attracting chemokines are proteins that induce chemotaxis, promote T cell differentiation, and cause tissue extravasation (28). Following several kinetic studies of chemokine treatments (not shown), we have identified the optimal protocol for recruiting high frequencies of protective T_{RM} cells into the lungs of CoV-Vacc-vaccinated mice. Chemokine treatments at the post-vaccination time points, days 10, 12, 14, 22, 24, 26, and the post-challenge time points, days 2, 4, 6, were identified as the optimal time points for chemokine treatment during the pre- and post-challenge with SARS-CoV-2. Our results are in agreement with previous reports on the prime/pull vaccine concept that increases homing and retaining the protective T_{RM} cells in the affected tissues (41–44).

In conclusion, the present study (i) validated previously unreported protective "ASYMP" epitopes that are potentially useful if included in a multi-epitope COVID-19 vaccine; (ii) characterizes the phenotype and the function of the protective $CD4^+$ and $CD8^+$ T cell sub-populations associated with immunologic control of SARS-CoV-2 infection, disease, and deaths; and (iii) demonstrates that bolstering the number of functional SARS-CoV-2-specific $CD4^+$ and $CD8^+$ T_{EM} and T_{RM} cells in the lungs through

the use of a SARS-CoV-2 human epitope/CXCL11-based prime/pull vaccine protected against SARS-CoV-2 infection, disease, and death. Thus, the prime/pull vaccine strategy provides an important new means of boosting lung-resident SARS-CoV-specific $CD4^+$ and $CD8^+$ memory T cell subsets for better outcomes against SARS-CoV-2 infection.

ACKNOWLEDGMENTS

The authors would like to thank the NIH Tetramer Facility (Emory University, Atlanta, GA) for providing the Tetramers used in this study. We also thank those who contributed directly or indirectly to the Next-Generation Universal Pan Coronavirus vaccine program at UC Irvine: UC Irvine Center for Clinical Research (CCR) and the Institute for Clinical & Translational Science (ICTS) for providing human blood samples used to select the epitopes used in this study. We thank Dr. Delia F. Tifrea for her continuous efforts and dedication in providing COVID-19 samples that are crucial for our clinical research. A special thanks to Gavin S. Herbert, Dr. Steven A. Goldstein, Dr. Michael J. Stamos, Jim Mazzo, Dr. Donald Forthal, and Dr. Garry Landucci for supporting UC Irvine Next-Generation Universal Pan Coronavirus vaccine program.

This work was supported by Public Health Service Research grants AI158060, AI150091, AI143348, AI147499, AI143326, AI138764, AI124911, and AI110902 from the National Institutes of Allergy and Infectious Diseases (NIAID) to L.B.M. and by R43AI174383 SBIR grant from NIAID to TechImmune, LLC.

AUTHOR AFFILIATIONS

[1]Laboratory of Cellular and Molecular Immunology, Gavin Herbert Eye Institute, School of Medicine, University of California Irvine, Irvine, California, USA
[2]Laboratory of Cell Biology and Molecular Genetics, Faculty of Sciences, Ibn Zohr University, Agadir, Morocco
[3]High containment facility, School of Medicine, University of California Irvine, Irvine, California, USA
[4]Department of Vaccines and Immunotherapies, TechImmune, LLC, University Lab Partners, Irvine, California, USA
[5]Department of Molecular Biology and Biochemistry, University of California Irvine, Irvine, California, USA
[6]Institute for Immunology, School of Medicine, University of California Irvine, Irvine, California, USA

AUTHOR ORCIDs

Latifa Zayou http://orcid.org/0009-0008-3049-4140
Swayam Prakash http://orcid.org/0000-0003-3986-890X
Lbachir BenMohamed http://orcid.org/0000-0001-9468-2521

FUNDING

Funder	Grant(s)	Author(s)
HHS | NIH | NIAID | Division of Intramural Research, National Institute of Allergy and Infectious Diseases (DIR, NIAID)	AI158060	Lbachir BenMohamed
HHS | NIH | National Institute of Allergy and Infectious Diseases (NIAID)	AI150091	Lbachir BenMohamed
HHS | NIH | National Institute of Allergy and Infectious Diseases (NIAID)	AI143348	Lbachir BenMohamed
HHS | NIH | National Institute of Allergy and Infectious Diseases (NIAID)	AI147499	Lbachir BenMohamed
HHS | NIH | National Institute of Allergy and Infectious Diseases (NIAID)	AI143326	Lbachir BenMohamed

Funder	Grant(s)	Author(s)
HHS | NIH | National Institute of Allergy and Infectious Diseases (NIAID)	AI138764	Lbachir BenMohamed
HHS | NIH | National Institute of Allergy and Infectious Diseases (NIAID)	AI124911	Lbachir BenMohamed
HHS | NIH | National Institute of Allergy and Infectious Diseases (NIAID)	AI110902	Lbachir BenMohamed

AUTHOR CONTRIBUTIONS

Latifa Zayou, Conceptualization, Data curation, Formal analysis, Methodology, Visualization, Writing – original draft | Swayam Prakash, Conceptualization, Data curation, Formal analysis, Funding acquisition, Methodology, Writing – original draft | Nisha Rajeswari Dhanushkodi, Methodology, Validation, Writing – original draft | Afshana Quadiri, Conceptualization, Data curation, Formal analysis, Methodology, Software, Validation, Visualization, Writing – original draft | Izabela Coimbra Ibraim, Resources | Mahmoud Singer, Methodology, Software | Amirah Salem, Methodology | Amin Mohammed Shaik, Methodology | Berfin Suzer, Methodology | Amruth Chilukuri, Methodology | Jennifer Tran, Methodology | Pauline Chau Nguyen, Methodology | Miyo Sun, Methodology | Kathy K. Hormi-Carver, Writing – original draft | Ahmed Belmouden, Resources, Writing – original draft | Hawa Vahed, Methodology | Daniel Gil, Writing – original draft | Jeffrey B. Ulmer, Writing – original draft, Writing – review and editing | Lbachir BenMohamed, Conceptualization, Data curation, Formal analysis, Funding acquisition, Investigation, Methodology, Project administration, Resources, Software, Supervision, Validation, Visualization, Writing – review and editing

ADDITIONAL FILES

The following material is available online.

Supplemental Material

Supplemental figures (JVI01096-23-s0001.pdf). Figures S1 to S3.
Supplemental table (JVI01096-23-s0002.pdf). Table S1.

REFERENCES

1. Zhu N, Zhang D, Wang W, Li X, Yang B, Song J, Zhao X, Huang B, Shi W, Lu R, Niu P, Zhan F, Ma X, Wang D, Xu W, Wu G, Gao GF, Tan W, China Novel Coronavirus Investigating and Research Team. 2020. A novel Coronavirus from patients with pneumonia in China, 2019. N Engl J Med 382:727–733. https://doi.org/10.1056/NEJMoa2001017
2. Singh D, Yi SV. 2021. On the origin and evolution of SARS-CoV-2. Exp Mol Med 53:537–547. https://doi.org/10.1038/s12276-021-00604-z
3. Tang X, Wu C, Li X, Song Y, Yao X, Wu X, Duan Y, Zhang H, Wang Y, Qian Z, Cui J, Lu J. 2020. On the origin and continuing evolution of SARS-CoV-2. Natl Sci Rev 7:1012–1023. https://doi.org/10.1093/nsr/nwaa036
4. Su W-L, Lu K-C, Chan C-Y, Chao Y-C. 2021. COVID-19 and the lungs: a review. J Infect Public Health 14:1708–1714. https://doi.org/10.1016/j.jiph.2021.09.024
5. Montazersaheb S, Hosseiniyan Khatibi SM, Hejazi MS, Tarhriz V, Farjami A, Ghasemian Sorbeni F, Farahzadi R, Ghasemnejad T. 2022. COVID-19 infection: an overview on cytokine storm and related interventions. Virol J 19:92. https://doi.org/10.1186/s12985-022-01814-1
6. Moss P. 2022. The T cell immune response against SARS-CoV-2. Nat Immunol 23:186–193. https://doi.org/10.1038/s41590-021-01122-w
7. Khalil BA, Elemam NM, Maghazachi AA. 2021. Chemokines and chemokine receptors during COVID-19 infection. Comput Struct Biotechnol J 19:976–988. https://doi.org/10.1016/j.csbj.2021.01.034
8. Callahan V, Hawks S, Crawford MA, Lehman CW, Morrison HA, Ivester HM, Akhrymuk I, Boghdeh N, Flor R, Finkielstein CV, Allen IC, Weger-Lucarelli J, Duggal N, Hughes MA, Kehn-Hall K. 2021. The pro-inflammatory chemokines CXCL9, CXCL10 and CXCL11 are upregulated following SARS-CoV-2 infection in an AKT-dependent manner. Viruses 13:1062. https://doi.org/10.3390/v13061062
9. Miller MC, Mayo KH. 2017. Chemokines from a structural perspective. Int J Mol Sci 18:2088. https://doi.org/10.3390/ijms18102088
10. Blot M, Jacquier M, Aho Glele L-S, Beltramo G, Nguyen M, Bonniaud P, Prin S, Andreu P, Bouhemad B, Bour J-B, Binquet C, Piroth L, Pais de Barros J-P, Masson D, Quenot J-P, Charles P-E, Pneumochondrie study group. 2020. CXCL10 could drive longer duration of mechanical ventilation during COVID-19 ARDS. Crit Care 24:632. https://doi.org/10.1186/s13054-020-03328-0
11. Sunagar R, Singh A, Kumar S. 2023. SARS-CoV-2: immunity, challenges with current vaccines, and a novel perspective on mucosal vaccines. Vaccines (Basel) 11:849. https://doi.org/10.3390/vaccines11040849
12. He X, Chen X, Wang H, Du G, Sun X. 2023. Recent advances in respiratory immunization: a focus on COVID-19 vaccines. J Control Release 355:655–674. https://doi.org/10.1016/j.jconrel.2023.02.011
13. Kingstad-Bakke B, Lee W, Chandrasekar SS, Gasper DJ, Salas-Quinchucua C, Cleven T, Sullivan JA, Talaat A, Osorio JE, Suresh M. 2022. Vaccine-induced systemic and mucosal T cell immunity to SARS-CoV-2 viral variants. Proc Natl Acad Sci U S A 119:e2118312119. https://doi.org/10.1073/pnas.2118312119
14. Prakash S, Srivastava R, Coulon P-G, Dhanushkodi NR, Chentoufi AA, Tifrea DF, Edwards RA, Figueroa CJ, Schubl SD, Hsieh L, Buchmeier MJ, Bouziane M, Nesburn AB, Kuppermann BD, BenMohamed L. 2021. Genome-wide B cell, $CD4^+$, and $CD8^+$ T cell epitopes that are highly conserved between human and animal Coronaviruses, identified from

SARS-CoV-2 as targets for preemptive pan-Coronavirus vaccines. J Immunol 206:2566–2582. https://doi.org/10.4049/jimmunol.2001438
15. Prakash S, Dhanushkodi NR, Zayou L, Ibraim IC, Quadiri A, Coulon PG, Tifrea DF, Suzler B, Amin M, Chilukuri A, Edwards RA, Vahed H, Nesburn AB, Kuppermann BD, Ulmer JB, Gil D, Jones TM, BenMohamed L. 2023. Cross-protection induced by highly conserved human B, CD4+, and CD8+ T cell epitopes-based Coronavirus vaccine against severe infection, disease, and death caused by multiple SARS-CoV-2 variants of concern. bioRxiv:2023.05.24.541850. https://doi.org/10.1101/2023.05.24.541850
16. Dhanushkodi N, Prakash S, Srivastava R, Coulon P-G, Vahed H, Zayou L, Quadiri A, Schaefer H, BenMohamed L. 2022. A prime/pull RR2/CXCL11 therapeutic vaccine that bolsters the number and function of dorsal root ganglia tissue-resident HSV-specific CD8$^+$ TRM cells protects latently infected Guinea pigs from recurrent genital herpes. bioRxiv. https://doi.org/10.1101/2022.07.22.501208
17. McCray PB, Pewe L, Wohlford-Lenane C, Hickey M, Manzel L, Shi L, Netland J, Jia HP, Halabi C, Sigmund CD, Meyerholz DK, Kirby P, Look DC, Perlman S. 2007. Lethal infection of K18-hACE2 mice infected with severe acute respiratory syndrome Coronavirus. J Virol 81:813–821. https://doi.org/10.1128/JVI.02012-06
18. Case JB, Bailey AL, Kim AS, Chen RE, Diamond MS. 2020. Growth, detection, quantification, and inactivation of SARS-CoV-2. Virology 548:39–48. https://doi.org/10.1016/j.virol.2020.05.015
19. Coulon P-G, Prakash S, Dhanushkodi NR, Srivastava R, Zayou L, Tifrea DF, Edwards RA, Cesar JF, Schubl SD, Hsieh L, Nesburn AB, Kuppermann BD, Bahraoui E, Vahed H, Gil D, Jones TM, Ulmer JB, BenMohamed L. 2022. High frequencies of PD-1$^+$Tim3$^+$TIGIT$^+$Ctla4$^+$ functionally exhausted SARS-CoV-2-specific CD4$^+$ and CD8$^+$ T cells associated with severe disease in critically ill COVID-19 patients. bioRxiv. https://doi.org/10.1101/2022.01.30.478343
20. Karcıoğlu O, Yüksel A, Baha A, Er AB, Esendağlı D, Gülhan PY, Karaoğlanoğlu S, Erçelik M, Şerifoğlu İ, Yıldız E, Köktürk N. 2020. Covid-19: the biggest threat of the 21st century: in respectful memory of the warriors all over the world. Turk Thorac J 21:409–418. https://doi.org/10.5152/TurkThoracJ.2020.20069
21. Sette A, Crotty S. 2022. Immunological memory to SARS-CoV-2 infection and COVID-19 vaccines. Immunol Rev 310:27–46. https://doi.org/10.1111/imr.13089
22. Sette A, Crotty S. 2021. Adaptive immunity to SARS-CoV-2 and COVID-19. Cell 184:861–880. https://doi.org/10.1016/j.cell.2021.01.007
23. Arieta CM, Xie YJ, Rothenberg DA, Diao H, Harjanto D, Meda S, Marquart K, Koenitzer B, Sciuto TE, Lobo A, et al. 2023. The T-cell-directed vaccine BNT162b4 encoding conserved non-spike antigens protects animals from severe SARS-CoV-2 infection. Cell 186:2392–2409. https://doi.org/10.1016/j.cell.2023.04.007
24. Karimabad MN, Kounis NG, Hassanshahi G, Hassanshahi F, Mplani V, Koniari I, Hung MY, Nadimi AE. 2021. The involvement of CXC motif chemokine ligand 10 (CXCL10) and its related chemokines in the pathogenesis of coronary artery disease and in the COVID-19 vaccination: a narrative review. Vaccines (Basel) 9:1224. https://doi.org/10.3390/vaccines9111224
25. Dörnte C, Traska V, Jansen N, Kostyra J, Baurmann H, Lauer G, Huang Y-J, Kramer S, Brauns O, Winkels H, Schmitz J, Dose C, Richter A, Schuster M. 2022. Vaccines against the original strain of SARS-CoV-2 provide T cell memory to the B.1.1.529 variant. Commun Med (Lond) 2:140. https://doi.org/10.1038/s43856-022-00203-7
26. Tincati C, Cannizzo ES, Giacomelli M, Badolato R, d'Arminio Monforte A, Marchetti G. 2020. Heightened circulating interferon-inducible chemokines, and activated pro-cytolytic Th1-cell phenotype features COVID-19 aggravation in the second week of illness. Front Immunol 11:580987. https://doi.org/10.3389/fimmu.2020.580987
27. Coperchini F, Chiovato L, Croce L, Magri F, Rotondi M. 2020. The cytokine storm in COVID-19: an overview of the involvement of the chemokine/chemokine-receptor system. Cytokine Growth Factor Rev 53:25–32. https://doi.org/10.1016/j.cytogfr.2020.05.003
28. Zlotnik A, Yoshie O. 2012. The chemokine superfamily revisited. Immunity 36:705–716. https://doi.org/10.1016/j.immuni.2012.05.008
29. Diniz MO, Mitsi E, Swadling L, Rylance J, Johnson M, Goldblatt D, Ferreira D, Maini MK. 2022. Airway-resident T cells from unexposed individuals cross-recognize SARS-CoV-2. Nat Immunol 23:1324–1329. https://doi.org/10.1038/s41590-022-01292-1
30. Almendro-Vázquez P, Laguna-Goya R, Paz-Artal E. 2023. Defending against SARS-CoV-2: the T cell perspective. Front Immunol 14:1107803. https://doi.org/10.3389/fimmu.2023.1107803
31. Srivastava R, Dhanushkodi N, Prakash S, Coulon PG, Vahed H, Zayou L, Quadiri A, BenMohamed L. 2022. High frequencies of phenotypically and functionally senescent and exhausted CD56$^+$CD57$^+$PD-1$^+$ natural killer cells, SARS-CoV-2-specific memory CD4$^+$ and CD8$^+$ T cells associated with severe disease in unvaccinated COVID-19 patients. bioRxiv. https://doi.org/10.1101/2022.07.26.501655
32. Kashte S, Gulbake A, El-Amin Iii SF, Gupta A. 2021. COVID-19 vaccines: rapid development, implications, challenges and future prospects. Hum Cell 34:711–733. https://doi.org/10.1007/s13577-021-00512-4
33. Krammer F. 2020. SARS-CoV-2 vaccines in development. Nature 586:516–527. https://doi.org/10.1038/s41586-020-2798-3
34. Cleary SJ, Pitchford SC, Amison RT, Carrington R, Robaina Cabrera CL, Magnen M, Looney MR, Gray E, Page CP. 2020. Animal models of mechanisms of SARS-CoV-2 infection and COVID-19 pathology. Br J Pharmacol 177:4851–4865. https://doi.org/10.1111/bph.15143
35. Renn M, Bartok E, Zillinger T, Hartmann G, Behrendt R. 2021. Animal models of SARS-CoV-2 and COVID-19 for the development of prophylactic and therapeutic interventions. Pharmacol Ther 228:107931. https://doi.org/10.1016/j.pharmthera.2021.107931
36. Park J-G, Pino PA, Akhter A, Alvarez X, Torrelles JB, Martinez-Sobrido L. 2022. Animal models of COVID-19: transgenic mouse model. Methods Mol Biol 2452:259–289. https://doi.org/10.1007/978-1-0716-2111-0_16
37. Joag V, Wijeyesinghe S, Stolley JM, Quarnstrom CF, Dileepan T, Soerens AG, Sangala JA, O'Flanagan SD, Gavil NV, Hong S-W, et al. 2021. Cutting edge: mouse SARS-CoV-2 epitope reveals infection and vaccine-elicited CD8 T cell responses. J Immunol 206:931–935. https://doi.org/10.4049/jimmunol.2001400
38. Esser MT, Marchese RD, Kierstead LS, Tussey LG, Wang F, Chirmule N, Washabaugh MW. 2003. Memory T cells and vaccines. Vaccine 21:419–430. https://doi.org/10.1016/s0264-410x(02)00407-3
39. Mosi L, Sylverken AA, Oyebola K, Badu K, Dukhi N, Goonoo N, Mante PK, Zahouli J, Amankwaa EF, Tolba MF, Fagbamigbe AF, de Souza DK, Matoke-Muhia D. 2021. Correlating WHO COVID-19 interim guideline 2020.5 and testing capacity, accuracy, and logistical challenges in Africa. Pan Afr Med J 39:89. https://doi.org/10.11604/pamj.2021.39.89.27522
40. Wu Z, Asokan A, Samulski RJ. 2006. Adeno-associated virus serotypes: vector toolkit for human gene therapy. Mol Ther 14:316–327. https://doi.org/10.1016/j.ymthe.2006.05.009
41. Shin H, Iwasaki A. 2012. A vaccine strategy that protects against genital herpes by establishing local memory T cells. Nature 491:463–467. https://doi.org/10.1038/nature11522
42. Wuest TR, Thapa M, Zheng M, Carr DJJ. 2011. CXCL10 expressing hematopoietic-derived cells are requisite in defense against HSV-1 infection in the nervous system of CXCL10 deficient mice. J Neuroimmunol 234:103–108. https://doi.org/10.1016/j.jneuroim.2011.03.006
43. Thapa M, Carr DJJ. 2009. CXCR3 deficiency increases susceptibility to genital herpes simplex virus type 2 infection: uncoupling of CD8+ T-cell effector function but not migration. J Virol 83:9486–9501. https://doi.org/10.1128/JVI.00854-09
44. Thapa M, Welner RS, Pelayo R, Carr DJJ. 2008. CXCL9 and CXCL10 expression are critical for control of genital herpes simplex virus type 2 infection through mobilization of HSV-specific CTL and NK cells to the nervous system. J Immunol 180:1098–1106. https://doi.org/10.4049/jimmunol.180.2.1098